KSCE Journal of Civil Engineering (2017) 21(6):2211-2225
DOI 10.1007/s12205-016-1386-4

Structural Engineering
pISSN 1226-7988, eISSN 1976-3808
www.springer.com/12205

Review of Analytical and Empirical Estimations for Incident Blast Pressure

Aleem Ullah*, Furqan Ahmad, Heung-Woon Jang***, Sung-Wook Kim****, and Jung-Wuk Hong*****

Received May 14, 2015/Revised August 9, 2016/Accepted October 30, 2016/Published Online December 12, 2016

Abstract

Recently, the blast load has become more recognized in the structural engineering field because the blast load can result in not only disproportionate structural failure but also tremendous casualties of lives and injuries. As an effort to overcome this problem, blast resistant analyses and designs have been developed, and the methodology would be incorporated into the conventional construction design. Analysis of structures exposed to blast load is the first step for the design, and it requires good understanding of blast phenomena and the following dynamic response of structures. This paper provides an up-to-date comprehensive review of the incident blast wave and its parameters for air and ground blasts. Considering the Unified Facilities Criteria (UFC 3-340-02) as a benchmark, a quantitative comparison between the empirical results presented by researchers and the result given in UFC charts is conducted for a span of scaled distances. We discuss the appropriate use of empirical or analytical equations for precise prediction of blast pressures, and recommend equations that match well the results presented in UFC.

Keywords: *blast wave, overpressure, arrival time, impulse, duration, scaled distance*

1. Introduction

The effect of explosion on a structure had not been studied comprehensively until World War II. Only limited amount of research work existed, and even it was kept classified considering its sensitivity to the general public (Hopkinson, 1915; Cranz, 1926). For the last several decades, the need of implementation of blast resistant design in major construction projects, especially for government buildings, had been recognized by observing numerous terrorists' attacks on civilian structures such as bombing in US embassy compound, Ankara (1958); US embassy attack, Beirut (1984); Alfred P. Murrah Federal Building attack, Oklahama (1995); World Trade Center attack, New York (2001); Mumbai attacks, Mumbai (2008); and Mariott Hotel attack, Islamabad (2008).

A large number of experimental and analytical studies were conducted during the second half of the 20th century to understand blast effects and structural response (Kinney and Graham, 1985; Henrych and Major, 1979; Brode, 1955; Mills, 1987; Kingery and Bulmash, 1984). The objective had been, firstly, to study the nature of the blast wave and the characteristics, and had evolved to investigate dominant factors affecting on the incident waves. Secondly, the aim had been to examine the response of a structure to blast loads (Beshara, 1994). Brode (1955) performed a numerical integration of the differential equations of gas motion in Lagrangian using von Neumann-Richtmyer artificial viscosity to avoid discontinuities and described dynamic and static pressures, positive and negative durations of pressure and velocity, and shock values (Brode, 1955). Henrych and Major (1979), based on the analysis of several experimental data, presented the formulae to compute peak positive overpressure, positive phase duration and positive phase impulse (Henrych and Major, 1979). Kinney and Graham (1985) utilized both experimental and theoretical means to get the parameters of the blast wave such as overpressure, positive phase duration, blast wave arrival time and positive phase impulse (Kinney and Graham, 1985). In 1984, Kingery and Bulmash presented the parameters for air burst in terms of high order polynomials (Kingery and Bulmash, 1984). Swisdak (1994) presented the same results, as were produced by Kingery, in terms of simplified polynomials with the results accurate to within 1% of the original Kingery values (Swisdak Jr., 1994). Wu and Hao (2005) developed empirical

*Jr. Structural Engineer, Redco International W.L.L, Precast Factory, Al Mesaieed, Qatar (E-mail: aleemullah@kaist.ac.kr)
**Assistant Professor, Dept. of Mechanical and Mechatronics, College of Engineering, Dhofar University, Salalah 211, P.O. Box 2509, Sultanate of Oman (E-mail: fahmad@du.edu.om)
***Ph.D. Candidate, Dept. of Civil and Environmental Engineering, Korea Advanced Institute of Science and Technology, Daejeon 34141, Korea (E-mail: hwjang90@kaist.ac.kr)
****Senior Research Fellow, Structural Engineering Research Institute, Korea Institute of Civil Engineering and Building Technology, Goyang, Korea (E-mail: swkim@kict.re.kr)
*****Member, Associate Professor, Dept. of Civil and Environmental Engineering, Korea Advanced Institute of Science and Technology, Daejeon 34141, Korea (Corresponding Author, E-mail: jwhong@alum.mit.edu, j.hong@kaist.ac.kr)

expressions of air blast pressure in the time domain as a function of surface explosion charge weight, distance to surface, and structure height. They also suggested functions for the ground shock time history spectral density, an envelop function, and a duration (Wu and Hao, 2005). There are several other researchers whose works related to blast wave parameters have been reported, and the representative achievements among those are explained in this review paper in the following sections.

The National Fire Protection Association's Guide to Fire and Explosion Investigation, NFPA 921 (2008), simply defines an explosion as "the sudden conversion of potential energy (chemical or mechanical) into kinetic energy with the production and release of gas under pressure. These high-pressure gases then do mechanical work such as moving, changing, or shattering nearby materials." An ideal blast wave profile can be completely defined using blast wave parameters such as blast wave arrival time (t_a), blast overpressure (P_s), positive phase duration (t_d), blast underpressure (P_s^-), negative phase duration (t_d^-), wave decay parameter (b), positive phase impulse (i_s), and negative phase impulse (i_s^-).

The steps for protecting the occupants of a building from the blast effect include defining of (a) the maximum charge weight used, (b) detonation locations, and (c) blast wave parameters. For the prediction of blast wave parameters from a high explosive detonation, unfortunately, the general engineering community has limited knowledge due to the nature of the explosives and the public security. The primary and widely used Unified Facilities Criteria (UFC 3-340-02) (2008) is open to public, and it contains blast wave parameter curves developed by Kingery and Bulmash for TNT bursts at standard atmospheric pressure and temperature. UFC presents two sets of conditions, of which one is for spherical bursts in free air and the other for hemispherical bursts at the ground surface.

For last few decades, many computer programs such as BLASTX, CTH, SHAMRC, FEFLO, FOIL, DYNA3D, ALE3D, LS-DYNA, Air3D, CONWEP, AUTODYN, ABAQUS, FEFLO, FOIL, and 3D BLAST have been developed to simulate the blast effects on structures. Computational methods used in these programs are generally categorized into two types: (a) those used for the prediction of blast loads on structures and (b) those for the calculation of structural response. Many of those can take into account the time varying load, nonlinear material properties, large displacement and the fluid-structure interaction (De Silva, 2010).

There are four types of explosions such as physical, chemical, electrical, and nuclear explosions. The physical explosion means the physical gas dynamic and thermodynamic effects including the bursting of a pressure vessel and/or a rapid phase transition. Chemical explosion involves exothermic reactions and combustion explosion from fuel (e.g., natural gas and propane). Electrical explosion occurs from an instantaneous release of electrical energy such as an arc event or other electrical failure (fault). Nuclear explosion is the result of military weapons based on nuclear fusion or fission of atomic nuclei (Pape *et al*., 2009). Explosive materials also might be classified considering their physical states (solid, liquid, or gas). On the other hand, military explosives are divided into two general classes, high and low explosives, according to their rate of decomposition. Solid explosives usually mean high explosives, and other materials such as flammable chemicals and propellants might be classified as low explosive materials. A variety of substances used in the manufactures of chemicals, fuels, and propellants are available in liquid or gaseous forms.

Blast loads on structures can be categorized into two major cases in terms of the confinement of the explosive charge

Table 1. Categories of Explosions Based on Confinement

Charge confinement	Category
Unconfined explosions	1. Free air blast (Spherical explosions) 2. Air burst 3. Surface burst (Hemispherical explosions)
Confined explosions	4. Fully vented
	5. Partially confined
	6. Fully confined

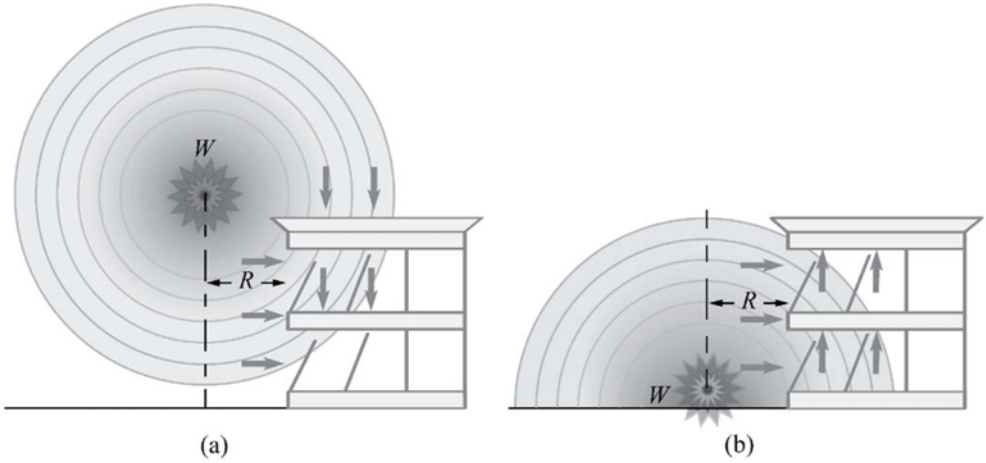

Fig. 1. Blast Pressure Effects on a Structure by: (a) Spherical, (b) Hemispherical Explosions

(unconfined and confined explosions), and the classifications might be further specified if the blast loading is generated within the structures or is imposed on the outer surface of structures. The detailed classification is summarized in Table 1 (Unified Facitilities Criteria 3-340-02, 2008). Spherical explosions (Fig. 1(a)) are defined as "an explosion, which occurs in free air, produces an initial output, whose shock wave propagates away from the center of the detonation, striking the protective structure without intermediate amplification of its wave." However, hemispherical explosions (Fig. 1(b)) are defined as: "a surface burst explosion will occur when the detonation is located close to or on the ground so that the initial shock is amplified at the point of detonation due to the ground reflections" (Unified Facitilities Criteria 3-340-02, 2008).

In this paper, a comprehensive review of analytical and empirical estimations for incident blast pressure is presented so that the interested practitioners and designers can understand, compute, and compare the blast wave profiles. Among several dozens of available equations, we selected most representative expressions by comparing with UFC curves, and the values by those equations are investigated and compared in this paper. The limitations of the representative empirical equations are explored, and the equations that yield closest value to that of UFC curves are suggested. Blast load is quite a broad topic. Therefore, to narrow down the scope, we investigate the incident pressure in unconfined spherical and hemispherical explosions generated by solid chemical explosives. Additionally, because much literature in this field is classified as confidential for security purpose, only a representative discussion is written down.

2. TNT Equivalence

Explosives can vary in both composition and detonation pressure. Each material is usually studied by the shattering effect of its sudden release of energy or blast pressure. Thus, in this review, we consider TNT as a reference explosive (Chock, 1999). The mass of an explosive other than TNT calculated by multiplying a conversion factor based on its specific energy and that of TNT. In addition to the amount of energy, other factors such as explosive material shape (flat, square, round, etc.), the number of explosive items, explosive confinement (casing, containers, etc.), and the pressure range (near, intermediate or far ranges) might affect the equivalency of the material compared to TNT (Unified Facitilities Criteria 3-340-02, 2008). TNT equivalents of some commonly used explosives are given in Table 2 (Mays and Smith, 1995; Bangash and Bangash, 2006). Mathematically, TNT equivalent charge is written as:

$$W = \frac{Q_x}{Q_{TNT}} W_x \tag{1}$$

where W is the equivalent charge in TNT, W_x is the mass of a particular explosive, Q_x is the mass specific energy of the particular explosive, and Q_{TNT} is the mass specific energy of TNT.

TNT equivalence is often estimated by the ratio of the two heats of explosives and TNT. However, it is also possible to compute TNT equivalence using the maximum overpressure or impulse (Esparza, 1986; Krauthammer, 2008; TM-855-1, 1986).

For the conservative estimation, it is recommended to increase TNT equivalent weight by 20% in order to compensate for unknown factors such as the variation of unexpected shock wave reflections, construction methods and quality of construction materials. This total charge weight is known as "effective charge weight" (Unified Facitilities Criteria 3-340-02, 2008).

Table 2. Conversion Factors for Explosives

Explosive	Mass specific energy $Q_x(kJ/kg)$	TNT equivalent Q_x/Q_{TNT}
Compound B (60% RDX 40% TNT)	5190	1.148
RDX (Cyclonite)	5360	1.185
HMX	5680	1.256
Nitroglycerin (liquid)	6700	1.481
TNT	4520	1.000
Blasting Gelatin (91% nitroglycerin, 7.9% nitrocellulose, 0.9% antacid, 0.2% water)	4520	1.000
60% Nitroglycerin dynamite	2710	0.600
Semtex	5660	1.250

3. Blast Scaling Law

Scaled parameters are determined from tests conducted in much smaller scales, and are used to predict the properties of large-scale explosions for various distances and energies (Conrath, 1999; Sachs, 1944). Hopkinson-Cranz blast scaling law, in the form of the cube root scaling, is the most commonly used blast scaling law. It was independently formulated by Hopkinson (1915) (Hopkinson, 1915) and Cranz (1926) (Cranz, 1926). In the law, self-similar blast waves are produced at identical scaled distances by detonating two explosive charges of similar geometry and of the same explosive but with different sizes in the same atmosphere. The scaled distance or the proximity factor (Z) in m/kg$^{1/3}$ is defined as (Mays and Smith, 1995; Uddin, 2010; UNODA, 2011):

$$Z = \frac{R}{W^{1/3}} \tag{2}$$

where R is the distance from the center of a spherical charge in meters (m), and W is the charge mass expressed in kilograms (kg) of TNT (Kim *et al*., 2009). Similarly, blast wave parameters such as the arrival time and positive and negative phase duration and impulse can be scaled using the Hopkinson-Cranz scaling law. Fig. 2 shows the Hopkinson-Cranz scaling law schematically.

A structure located at a distance (R) from a charge of diameter (d) will be subjected to a blast wave of the peak overpressure (P), positive phase duration (t_d), and impulse (i_s). Hopkinson-Cranz scaling law then states that a structure located at a distance (λR)

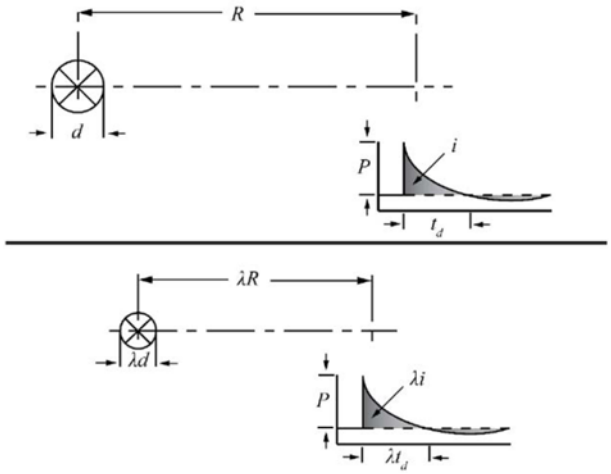

Fig. 2. Hopkinson-Cranz blast scaling law

from the center of a charge of diameter (λd) will experience a blast wave of a typical form with amplitude (P), duration (λt_d) and impulse (λi_s). All characteristic times are modified by the same factor (λ) as that of length (Conrath, 1999).

4. Profiles of Blast Waves

After detonation of a high explosive in free air, the expansion of the hot gases at extremely high pressure causes a shock wave that moves outward at a high velocity. The pressure-time history of an idealized explosion at a fixed distance (R) from the center of the explosion can be described as shown in Fig. 3, which is called the Friedlander waveform. The pressure-time history can be divided into positive and negative phases. The ideal Friedlander waveform has blast wave parameters such as the arrival time (t_a), peak positive overpressure (P_s), positive duration (t_d), under or negative pressure (P_s^-), negative duration (t_d^-), wave decay parameter (b), positive impulse (i_s), and negative impulse (i_s^-), all of which are discussed in detail in the following sections.

For the study of blast wave effects on structures and also for the design of structures or components (Table 3 shows

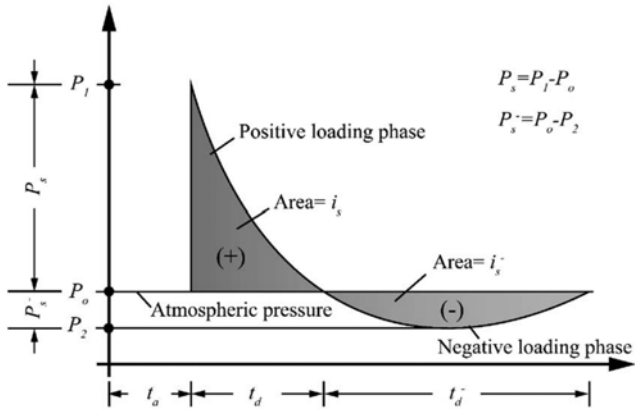

Fig. 3. Ideal Temporal Pressure Profile Resulting from Explosion in Air

Table 3. Expected Shock Wave Effects on Objects

Overpressure (MPa × 10^{-3})	Expected damage
1.0-1.5	Window glass cracks
3.5-7.6	Minor damage in some buildings
7.6-12.4	Metal panels deformed
12.4-20	Concrete walls damaged
Over 35	Wooden buildings demolished
27.5-48	Major damage to steel objects
40-60	Heavy damage to reinforced concrete buildings
70-80	Probable demolition of most buildings

expected effects of a shock waves on objects (Kinney and Graham, 1985)), the positive phase is typically considered more important than the negative phase because of the large amplitude of the overpressure (P_s) and the concentrated impulse (i_s) (Uddin, 2010). On the other hand, the negative phase has often been ignored because the magnitude is relatively small, and is difficult to be measured (Nassr, 2012). However, some studies have shown that, for scaled distances (Z) larger than 20 m/kg$^{1/3}$ (especially for scaled distances (Z) larger than 50 m/kg$^{1/3}$), the influence of the negative phase cannot be neglected (Larcher, 2008). In addition, for relatively flexible structures, the negative phase pressure might be included (Uddin, 2010).

4.1 Positive Phase/Shock Wave

In the positive phase, the shock wave travels along a point of consideration after detonation of an explosive in a time interval, the so-called arrival time (t_a). An instantaneous increase in the ambient pressure occurs due to the highly compressed air of the shock front, and the pressure reaches its peak value, which is known as the incident peak pressure or peak overpressure (P_s). After reaching the peak, pressure decays back to normal atmospheric pressure (P_o) over a period known as the positive phase duration (t_d). The area under the pressure-time pulse over the positive phase is referred to as the positive incident impulse (i_s) (Larcher, 2008). Blast pressure variation is the difference of the peak overpressure (P_s) and negative pressure (P_s^-). For the calculation and presentation of positive blast pressure profiles, numerous expressions have been proposed. Flynn proposed a linear decaying pressure profile, which is given by (Chock, 1999):

$$P(t) = P_o + P_s\left(1 - \frac{t}{t_d}\right), \quad 0 < t \le t_d \tag{3}$$

Considering the decaying nature of blast profile, a better form was presented by Ethridge in his 1965 work (Chock, 1999):

$$P(t) = P_o + P_s e^{-ct} \tag{4}$$

where t is measured from the time of arrival (t_a). The curve fitting of Eq. (4) can be performed using the peak overpressure and the wave decay rate as parameters. The next extension of this process is to fit experimental results with three different parameters.

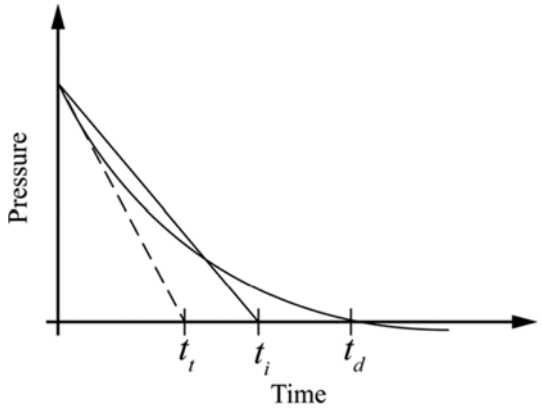

Fig. 4. Triangular Pressure-time Profile

This form is usually called as the modified Friedlander's equation, which is expressed as (Chock, 1999; Kangarlou, 2013; Kadid *et al*., 2012):

$$P(t) = P_o + P_s\left(1-\frac{t}{t_d}\right)e^{-bt/t_d} \tag{5}$$

where b is the decay coefficient. For the simplicity, the blast profile can by approximated by the linearly decaying triangular pulses shown in Fig. 4. This linearly decaying triangular profiles have the same initial peak overpressure, but have different durations depending on the expected time of maximum structural response (Beshara, 1994; Chock, 1999).

4.1.1 Overpressure

Several empirical relations have been presented in literature to predict blast overpressure based on the analysis of large sets of experimental data at different scaled distances and charge sizes. The formulae for a spherical TNT explosion in air can be used for hemispherical explosions with increasing the explosive weight by multiplying a reflection factor, 2η. The coefficient (η) accounts for the energy used for deformation of the base material, and the values for different base materials are listed in Table 4 (Jeremić and Bajić, 2006).

On the other hand, Unified Facilities Criteria (Unified Facitilities Criteria 3-340-02, 2008) is widely used as a reference for the design of protective structures. Figs. 5(a) and (b) show positive phase wave parameters for a spherical explosion in free air and for a hemispherical TNT explosion on the ground, respectively (Unified Facitilities Criteria 3-340-02, 2008).

The empirical and analytical equations for spherical airbursts presented by several researchers are given below. These presented equations have been modified to have the unit of megapascals (MPa), while W is expressed in kg and Z in m/kg$^{1/3}$.

Sadovskyi (1952) (Kangarlou, 2013; Jeremić and Bajić, 2006; Chang and Young, 2010, Sadovskiy, 2004)

$$P_s = \frac{0.085}{Z}+\frac{0.3}{Z^2}+\frac{0.82}{Z^3} \tag{6}$$

Brode (1955) (Brode, 1955; Mays and Smith, 1995; Kadid *et al*., 2012; Chang and Young, 2010; Yin *et al*., 2009; Abdollahzadeh and Nemati, 2013; Low and Hao, 2001; Smith and Hetherington, 1994)

$$P_s = \begin{cases} \dfrac{0.67}{Z^3}+0.1 & \text{for } (1 < P_s) \\ \dfrac{0.0975}{Z}+\dfrac{0.1455}{Z^2}+\dfrac{0.585}{Z^3}-0.0019 & \text{for } (0.01 \le P_s \le 1) \end{cases} \tag{7}$$

Naumyenko and Petrovskyi (1956) (Henrych and Major, 1979;

Table 4. Values of the Coefficient η for Various Base Materials

Type of material	Steel plate	Reinforced concrete plate	Concrete, rock	Compact sandy clay; Clay	Medium compact soil	Water
η	1	0.95-1	0.85-0.9	0.7-0.8	0.6-0.65	0.55-0.6

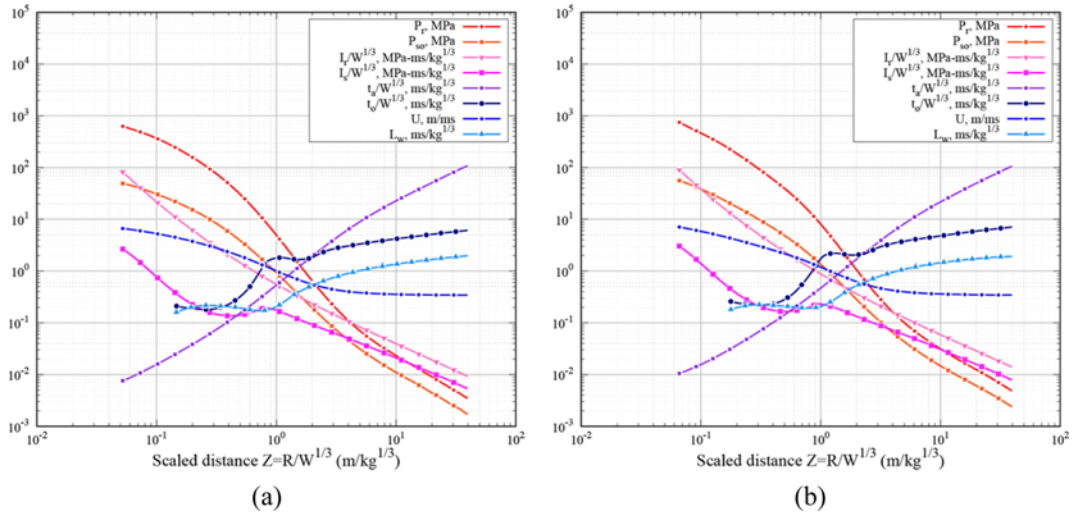

Fig. 5. Positive Phase Parameters for: (a) Spherical, (b) Hemispherical TNT Explosions

Low and Hao, 2001)

$$P_s = \begin{cases} \dfrac{1.050}{Z^3} - 0.0981 & \text{for}\left(Z \le 1\right) \\ \dfrac{0.0745}{Z} + \dfrac{0.250}{Z^2} + \dfrac{0.637}{Z^3} & \text{for}\left(1 < Z \le 15\right) \end{cases} \tag{8}$$

Adushkin and Korotkov (1961) (Adushkin and Korotkov, 1961; Pierre-Emmanuel Sauvan, 2012)

$$P_s = \frac{0.08}{Z} + \frac{0.28}{Z^2} - \frac{0.322}{Z^3} \qquad \text{for}\left(0.8 \le Z < 18\right) \tag{9}$$

Henrych and Major (1979) (Henrych and Major, 1979; Kangarlou, 2013; Kadid, Nezzar and Yahiaoui, 2012; Yin *et al*., 2009; Abdollahzadeh and Nemati, 2013; Low and Hao, 2001; Saska *et al*., 2011)

$$P_s = \begin{cases} \dfrac{1.380}{Z} + \dfrac{0.543}{Z^2} - \dfrac{0.035}{Z^3} + \dfrac{0.000613}{Z^4} & \text{for}\,(0.05 \le Z \le 0.3) \\ \dfrac{0.607}{Z} - \dfrac{0.032}{Z^2} + \dfrac{0.209}{Z^3} & \text{for}\,(0.3 < Z \le 1) \\ \dfrac{0.0649}{Z} + \dfrac{0.397}{Z^2} + \dfrac{0.322}{Z^3} & \text{for}\,(1 < Z \le 10) \end{cases} \tag{10}$$

Held (1983) (Chang and Young, 2010; Held, 1983; Goel *et al*., 2012)

$$P_s = 2\frac{W^{2/3}}{R^2} \tag{11}$$

Kinney and Graham (1985) (Kinney and Graham, 1985; Nassr, 2012; Larcher, 2008; Kangarlou, 2013)

Kinney and Graham's equation does not use any polynomial base; therefore, this equation does not have limits on the valid range.

$$P_s = P_o \frac{808\left[1 + \left(\dfrac{Z}{4.5}\right)^2\right]}{\sqrt{\left[1 + \left(\dfrac{Z}{0.048}\right)^2\right]} \times \sqrt{\left[1 + \left(\dfrac{Z}{0.32}\right)^2\right]} \times \sqrt{\left[1 + \left(\dfrac{Z}{1.35}\right)^2\right]}} \tag{12}$$

Mills (1987) (Kadid, Nezzar and Yahiaoui, 2012; Chang and Young, 2010; Low and Hao, 2001; Vijayaraghavan *et al*., 2012)

$$P_s = \frac{1.772}{Z^3} - \frac{0.114}{Z^2} + \frac{0.108}{Z} \tag{13}$$

Hopkins-Brown and Bailey (1998) (Hopkins-Brown and Bailey, 1998)

$$P_s = \begin{cases} -1.245 + \dfrac{1.935}{Z} + \dfrac{0.2353}{Z^2} - \dfrac{0.01065}{Z^3} & \text{for}\left(0.05 \le Z \le 1.15\right) \\ \dfrac{0.0707}{Z} + \dfrac{0.3602}{Z^2} + \dfrac{0.4891}{Z^3} & \text{for}\left(1.15 < Z \le 40\right) \end{cases} \tag{14}$$

Gelfand and Silnikov (2004) (Gelfand and Silnikov, 2004)

$$P_s = \begin{cases} 1.7 \times 10^3 \exp(-7.5 \times Z^{0.28}) + 0.0156 & \text{for}\left(0.1 \le Z < 8\right) \\ 8 \times 10^3 \exp(-10.7 \times Z^{0.1}) & \text{for}\left(8 \le Z\right) \end{cases} \tag{15}$$

Bajić (2007) (Bajić, 2007)

$$P_s = 0.102\frac{W^{1/3}}{R} + 0.436\frac{W^{2/3}}{R^2} + 1.4\frac{W}{R^3} \tag{16}$$

National Defense Engineering Design Specifications (NDEDS), China (Li and Ma, 1992)

$$P_s = 0.084\left(\frac{\sqrt[3]{W}}{R}\right) + 0.27\left(\frac{\sqrt[3]{W}}{R}\right)^2 + 0.7\left(\frac{\sqrt[3]{W}}{R}\right)^3 \tag{17}$$

For hemispherical surface bursts, the empirical formulae for the peak overpressure proposed by different researchers are summarized below. All the equations have been modified to have the unit of megapascals (MPa).

Newmark and Hansen (1961) (Kadid *et al*., 2012; Vijayaraghavan *et al*., 2012; Newmark and Hansen, 1961)

$$P_s = 0.6784\frac{W}{R^3} + 0.294\left(\frac{W}{R^3}\right)^{1/2} \tag{18}$$

Wu and Hao (2005) (Wu and Hao, 2005)

$$P_s = \begin{cases} 1.059\left(\dfrac{R}{W^{1/3}}\right)^{-2.56} - 0.051 & \text{for}\left(0.1 \le \dfrac{R}{W^{1/3}} \le 1\right) \\ 1.008\left(\dfrac{R}{W^{1/3}}\right)^{-2.01} & \text{for}\left(1 < \dfrac{R}{W^{1/3}} \le 10\right) \end{cases} \tag{19}$$

Ahmad *et al*. (2012) (Ahmad *et al*., 2014)

$$P_s = 2.46\left(\frac{R}{W^{1/3}}\right)^{-2.67} \tag{20}$$

Siddiqui and Ahmad (2007) (Ahmad *et al*., 2014)

$$P_s = 1.017\left(\frac{R}{W^{1/3}}\right)^{-1.91} \quad \text{for}\left(1 \le \frac{R}{W^{1/3}} \le 12\right) \tag{21}$$

Iqbal and Ahmad (2009) (Iqbal and Ahmad, 2009)

$$P_s = 1.026\left(\frac{R}{W^{1/3}}\right)^{-1.96} \quad \text{for}\left(1 \le \frac{R}{W^{1/3}} \le 12\right) \tag{22}$$

Ahmad *et al*. (2012a) (Ahmad *et al*., 2012)

$$P_s = 1.5956\left(\frac{R}{W^{1/3}}\right)^{-2.868} \quad \text{for}\left(R < 5\right) \tag{23}$$

Table 5. Simplified Kingery Air Blast Coefficients for Blast Overpressure

Z (m/kg$^{1/3}$)	A_1	B_1	C_1	D_1	E_1	F_1	G_1
0.2-2.9	7.2106	-2.1069	-0.3229	0.1117	0.0685	0	0
2.9-23.8	7.5938	-3.0523	0.40977	0.0261	-0.01267	0	0
23.8-198.5	6.0536	-1.4066	0	0	0	0	0

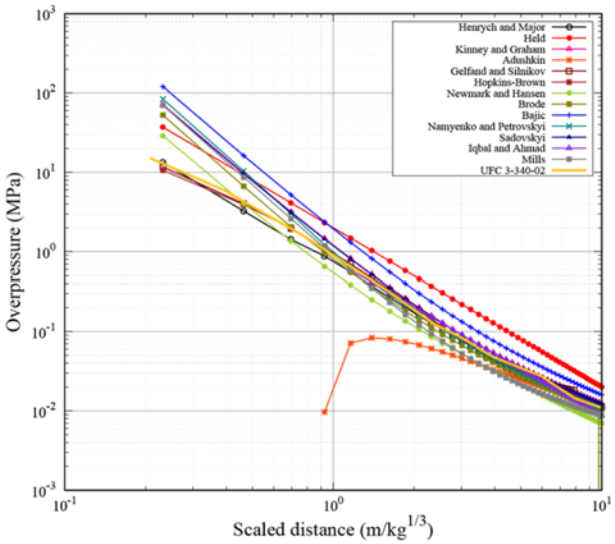

Fig. 6. Comparison of Positive Overpressure Computed by Empirical Formulae and UFC 3-340-02 (Fig. 5(a))

Table 6. Values of Parameters at Sea Level

Temperature (°C)	Air density (kg/m^3)	Ambient pressure (MPa)	Height above sea level	Sound speed (m/s)
15	1.225	0.101325	0	340

Swisdak (1994) (Swisdak Jr., 1994)

$$P_s = \exp((A_1 + B_1 \times (\ln(Z)) + C_1 \times (\ln(Z))^2 + D_1 \times (\ln(Z))^3 + E_1 \times (\ln(Z))^4 + F_1 (\ln(Z))^5 \times G_1 (\ln(Z))^6) \times 10^{-3} \quad (24)$$

where Z is the scaled range and A_1, B_1, C_1, D_1, F_1, and G_1 are the simplified Kingery air blast coefficients given in Table 5. All of the Swisdak's equations uses Kingery air blast coefficients. In addition to these empirical relations, there exist other experimental diagrams presented by Kingery and Bulmash, and Baker. Kingery and Bulmash suggested diagrams valid up to Z = 40 m/kg$^{1/3}$, while Baker's diagram covers up to Z = 1000 m/kg$^{1/3}$. Fig. 6 shows the log-log plot of overpressure versus scaled distance (Z) in the conditions listed in Table 6 for spherical air bursts. To compare the pressures quantitatively, the empirical relations by hemispherical burst are converted to that of the spherical burst for a steel plate which has the reflection factor of 2. The pressures calculated from the above empirical relations are compared with the results by UFC 3-340-02 (2008). The difference between the empirical relations and UFC charts is significant, especially in the range of (0.2 < Z (m/kg$^{1/3}$) < 1.0) while the variation is negligible for (Z (m/kg$^{1/3}$) > 1.0.) It means that overpressure at large distances from an explosive charge can be predicted with reasonable confidence by means of empirical equations. However, when the charge is close to a target, the result might not be accurate. Bajic's equation (Eq. (16)) gives the largest values, and the equation by Gelfand and Silnikov (Eq. (15)) gives the smallest values. The empirical equation by Kinney and Graham (Eq. (12)) give the values very close to the result by UFC.

4.1.2 Arrival Time of Blast Wave

The empirical relations for the arrival time (t_a) of a shock wave front from the center of an explosion to a structure are not commonly available and are not usually included in most studies. In this review, the arrival time formulas given by different researchers are summarized. All equations presented have been modified to have the unit of milliseconds (ms).

Kinney and Graham (1985) (Kinney and Graham, 1985)

$$t_a = \frac{1}{a_o}\int_{r_c}^{R}\left[\frac{1}{1+\frac{6P_s}{7P_o}}\right]^{1/2} dR = \frac{1}{a_o}\int_{r_c}^{R}\left(\frac{1}{M_x}\right)dR \quad (25)$$

where a_o is the speed of sound in the undisturbed atmosphere, M_x is the Mach number and r_c is the charge radius. The given integration equation can be calculated using the graphical method, but this method is less precise than numerical calculation. For example, in order to calculate the arrival time using the graphical method (Kinney and Graham, 1985), the overpressures (P_s) (using Eq. (12)) at different scaled distances are converted into Mach numbers (M_x) and substituted into Eq. (25). Reciprocals of the Mach number against the distance are plotted in Fig. 7. The curve is extrapolated to the charge radius (0.227 m) and the area under the curve to the distance of 20 m is calculated as 18.866 m. Dividing by the speed of sound, 340 m/s, the arrival time is obtained as 58.8 ms. The expression for the arrival times are listed:

Swisdak (1994) (Swisdak Jr., 1994)

$$t_a = \exp(A_2 + B_2 \times (\ln(Z)) + C_2 \times (\ln(Z))^2 + D_2 \times (\ln(Z))^3 + E_2 \times (\ln(Z))^4 + F_2 \times (\ln(Z))^5 + G_2 \times (\ln(Z))^6) \times W^{1/3} \quad (26)$$

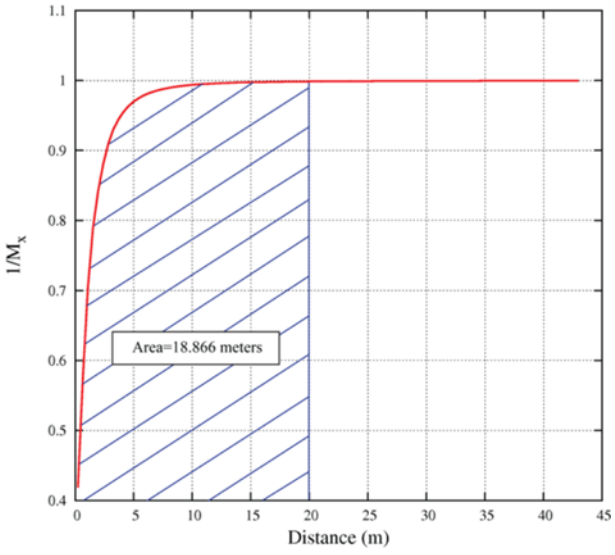

Fig. 7. Estimation of Arrival Time

Table 7. Simplified Kingery Air Blast Coefficients for Blast Arrival Time

Z (m/kg$^{1/3}$)	A_2	B_2	C_2	D_2	E_2	F_2	G_2
0.06-1.50	-0.7604	1.8058	0.1257	-0.0437	-0.0310	-0.00669	0
1.50-40	-0.7137	1.5732	0.5561	-0.4213	0.1054	-0.00929	0

where Z is the scaled range and A_2, B_2, C_2, D_2, F_2, and G_2 are the simplified Kingery air blast coefficients as given in Table 7.

Wu and Hao (2005) (Wu and Hao, 2005)

$$t_a = 0.34\frac{R^{1.4}W^{-0.2}}{a_o} \tag{27}$$

where a_o is the speed of sound in air, given in Table 6.

Iqbal and Ahmad (2009) (Iqbal and Ahmad, 2009)

$$t_a = 560\frac{R^{1.4}W^{-0.2}}{a_o} \tag{28}$$

Ahmad *et al*. (2012a) (Ahmad *et al*., 2012)

$$t_a = \frac{4637}{a_o}\left(\frac{R}{W^{1/3}}\right)^{-0.138} \tag{29}$$

Ahmad *et al*. (2014) (Ahmad *et al*., 2014)

$$t_a = \frac{8534}{a_o}\left(\frac{R}{W^{1/3}}\right)^{-0.996} \tag{30}$$

Figure 8 shows the standard doubly logarithmic plot of the blast arrival time (t_a) with respect to the scaled distance (Z). The variation among the results produced by the equations given by researchers is larger in the region ($0.2 < Z$ (m/kg$^{1/3}$) < 1) while it is smaller for the scaled distance range (Z (m/kg$^{1/3}$) > 1). The results obtained from Wu and Hao's equation (Eq. (27)) show closer agreement with the UFC chart values. On the other hand,

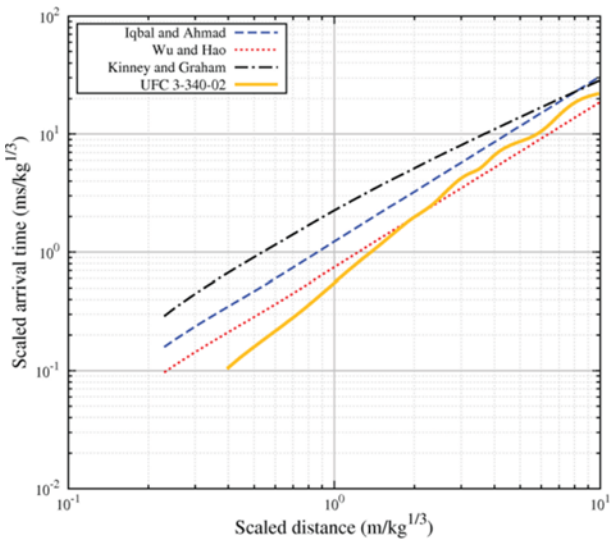

Fig. 8. Comparison of Scaled Arrival Time Computed by Empirical Formulae and UFC 3-340-02

Kinney and Graham's equation (Eq. (25)) produces the largest values among all the presented empirical equations.

4.1.3 Positive Phase Duration

The duration of a blast wave might be defined as the time difference between the passing of the shock front and the passing of the end of the positive pressure phase (Goel, Matsagar, Gupta and Marburg, 2012). The positive phase duration might be calculated using the scaled distance (Z), or the mass of charge (W) and the standoff distance (R). Several empirical relations of positive phase duration (t_d) are listed, and equations are modified to have the unit of milliseconds (ms) as follows:

Sadovskyi (1952) (Kangarlou, 2013; Jeremić and Bajić, 2006; Sadovskiy, 2004)

$$t_d = 1.2\sqrt[6]{W}\sqrt{R} \tag{31}$$

Newmark (1972) (Beshara, 1994; Newmark and Hansen, 1961)

For a surface burst, the total positive phase duration of blast overpressure is expressed in milliseconds (ms) as:

$$t_d = 10\cdot W^{1/3} \tag{32}$$

Henrych (1979) (Henrych and Major, 1979)

$$t_d = W^{1/3}(0.107 + 0.444Z + 0.264Z^2 - 0.129Z^3 + 0.0335Z^4) \quad \text{for } (0.05 \le Z \le 3) \tag{33}$$

Kinney and Graham (1985) (Beshara, 1994; Nassr, 2012; Kangarlou, 2013)

$$t_d = \frac{980\left[1+\left(\frac{Z}{0.54}\right)^{10}\right]}{\left[1+\left(\frac{Z}{0.02}\right)^{3}\right]\left[1+\left(\frac{Z}{0.74}\right)^{6}\right]\sqrt{1+\left(\frac{Z}{6.9}\right)^{2}}}W^{1/3} \tag{34}$$

Swisdak (1994) (Swisdak Jr., 1994)

$$t_d = \exp(A_3 + B_3(\ln(Z)) + C_3\times(\ln(Z))^2 + D_3\times(\ln(Z))^3 + E_3\times(\ln(Z))^4 + F_3\times(\ln(Z))^5 + G_3\times(\ln(Z))^6)\times W^{1/3} \tag{35}$$

where Z is the scaled range and A_3, B_3, C_3, D_3, F_3, and G_3 are the simplified Kingery air blast coefficients, given in Table 8.

Smith (Lam *et al*., 2004)

$$t_d \approx W^{1/3}\times 10^{0.25+0.27\log_{10}\left(\frac{R}{W^{1/3}}\right)} \tag{36}$$

Wu and Hao (2005) (Wu and Hao, 2005)

$$t_d = 1.9\left(\frac{R}{W^{1/3}}\right)^{1.30} + 0.5\left(\frac{R}{W^{1/3}}\right)^{0.72} W^{0.4} \tag{37}$$

Table 8. Simplified Kingery Air Blast Coefficients for Positive Phase Duration

Z (m/kg$^{1/3}$)	A_3	B_3	C_3	D_3	E_3	F_3	G_3
0.2-1.02	0.5426	3.2299	-1.5931	-5.9667	-4.0815	-0.9149	0
1.02-2.80	0.5440	2.7082	-9.7354	14.3425	-9.7791	2.8535	0
2.80-40	-2.4608	7.1639	-5.6215	2.2711	-0.44994	0.03486	0

Iqbal and Ahmad (2009) (Iqbal and Ahmad, 2009)

$$t_d = 4.6\left(\frac{R}{W^{1/3}}\right)^{0.92} + 1.3\left(\frac{R}{W^{1/3}}\right)^{0.89} W^{0.52} \tag{38}$$

Ahmad *et al*. (2012a) (Ahmad *et al*., 2012)

$$t_d = 0.3108\left(\frac{R}{W^{1/3}}\right)^{-0.1} + 2.462\left(\frac{R}{W^{1/3}}\right)^{-0.472} \tag{39}$$

Izadifard and Maheri (Izadifard and Foroutan, 2010)

$$t_d = \begin{cases} W^{1/3}\times(-64.86Z^4+52.32Z^3-15.68Z^2+1.794Z+0.1034) & \text{for}(Z\le 0.37) \\ W^{1/3}\times(4.64Z^2-3.86Z+0.854) & \text{for}(0.37<Z\le 0.82) \\ W^{1/3}\times(-2.97X^3+6.27X^2+0.358X+0.763) & \text{for}(0.82<Z\le 2.5) \\ W^{1/3}\times(0.608X^3-2.38^2+5.62X-0.22) & \text{for}(2.5<Z) \end{cases} \tag{40}$$

where $X = \log_{10}(Z)$ (41)

Ahmad *et al*. (2014) (Ahmad *et al*., 2014)

$$t_d = 1.4\left(\frac{R}{W^{1/3}}\right)^{-0.759} + 0.5\left(\frac{R}{W^{1/3}}\right)^{2.159} \tag{42}$$

Positive phase duration computed by above empirical relations show dissimilar behaviors (Fig. 9). Therefore it is hard to predict the trend of positive phase duration, plotted against scaled distance. However, it should be noted that the variation in values of the duration is larger for the scaled distance range (0.2< Z (m/kg$^{1/3}$)<1) and becomes negligible for the range (Z (m/kg$^{1/3}$)>1). Iqbal and Ahmad's equation (Eq. (38)) gives the largest value, while Kinney and Graham's equation (Eq. (33)) yields the smallest over most of the range. Sadovskyi's equation (Eq. (30)) calculates values relatively closer to the UFC values.

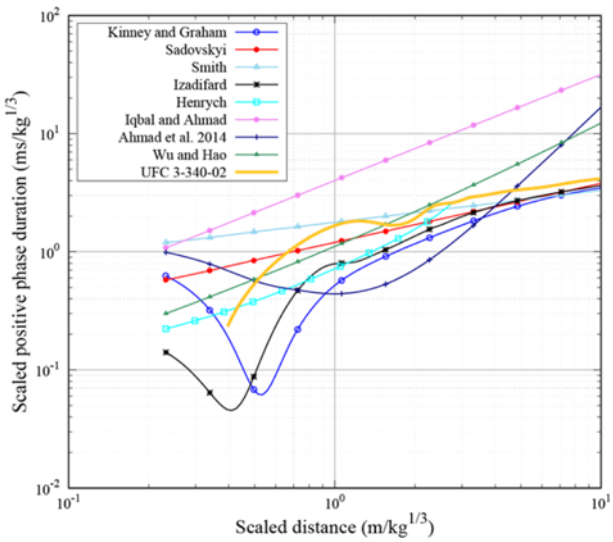

Fig. 9. Comparison of Scaled Positive Phase Duration Computed by Empirical Formulae and UFC 3-340-02

4.1.4 Positive Phase Impulse

The incident overpressure impulse can be calculated by integrating pressure-time curve over the positive phase duration (t_d). The positive impulse is the parameter that has central importance for the loading of a structure and can be mathematically expressed as (Kinney and Graham, 1985):

$$i_s = \int_{t_a}^{t_a+t_d} [P(t) - P_o]\,dt \tag{43}$$

Positive impulse also can be calculated using scaled distance (Z) or mass of charge (W) and standoff distance (R). All equations presented have been modified to have units of pascal-second (Pa-s). Several empirical relations of positive phase impulse (i_s) are listed below:

Sadovskyi (1952) (Henrych and Major, 1979; Kangarlou, 2013; Jeremić and Bajić, 2006; Chang and Young, 2010; Sadovskiy, 2004; Saska *et al*., 2011)

$$i_s = 200\frac{\sqrt[3]{W^2}}{R} \tag{44}$$

and

$$i_s = \begin{cases} (34\sim 36)\times 9.81\times\dfrac{\sqrt[3]{W^2}}{R} & \text{for}(Z>0.5) \\ 147.15\times\dfrac{W}{R^2} & \text{for}(Z<0.25) \end{cases} \tag{45}$$

Henrych (1979) (Henrych and Major, 1979; Saska *et al*., 2011)

$$i_s = \begin{cases} 9.81\times W^{1/3}\left(663-\dfrac{1115}{Z}+\dfrac{629}{Z^2}-\dfrac{100.4}{Z^3}\right) & for(0.4\le Z\le 0.75) \\ 9.81\times W^{1/3}\left(-32.2+\dfrac{211}{Z}-\dfrac{216}{Z^2}+\dfrac{80.1}{Z^3}\right) & for(0.75<Z\le 3) \end{cases} \tag{46}$$

Held (1983) (Chang and Young, 2010; Held, 1983)

$$i_s = 300\frac{W^{2/3}}{R} \tag{47}$$

Kinney and Graham (1985) (Kinney and Graham, 1985;

Table 9. Simplified Kingery Air Blast Coefficients for Positive Phase Impulse

Z (m/kg$^{1/3}$)	A_4	B_4	C_4	D_4	E_4	F_4	G_4
0.2-0.96	5.522	1.117	0.6	-0.292	-0.087	0	0
0.96-2.38	5.465	-0.308	-1.464	1.362	-0.432	0	0
2.38-33.7	5.2749	-0.4677	-0.2499	0.0588	-0.00554	0	0
33.7-158.7	5.9825	-1.062	0	0	0	0	0

Nassr, 2012; Larcher, 2008; Kangarlou, 2013)

$$i_s = \frac{6.7\sqrt{1+(Z/0.23)^4}}{Z^2\sqrt[3]{1+(Z/1.55)^3}} W^{1/3} \tag{48}$$

Swisdak (1994) (Swisdak Jr., 1994)

$$i = \exp(A_4 + B_4 \times (\ln(Z)) + C_4 \times (\ln(Z))^2 + D_4 \times (\ln(Z))^3 \\ E_4 \times (\ln(Z))^4 + F_4 \times (\ln(Z))^5 + G_4 \times (\ln(Z))^6) \times W^{1/3} \tag{49}$$

where Z is the scaled range and A_4, B_4, C_4, D_4, F_4, and G_4 are the simplified Kingery air blast coefficients, given in Table 9.

Hopkins-Brown and Bailey (1998) (Hopkins-Brown and Bailey, 1998)

$$i_s = \begin{cases} W^{1/3}\left(308.2 - \frac{106.65}{Z} + \frac{18.89}{Z^2} - \frac{0.401}{Z^3}\right) & \text{for}\,(0.05 \le Z \le 1.15) \\ W^{1/3}\left(1.79 + \frac{196.0}{Z} + \frac{8.62}{Z^2} + \frac{30.5}{Z^3}\right) & \text{for}\,(1.15 < Z \le 40) \end{cases} \tag{50}$$

Figure 10 shows the log-log plot of the positive phase impulse versus the scaled distance (Z). The variation among positive phase impulse values is larger for scaled distances (0.2 < Z (m/kg$^{1/3}$) < 1) and smaller for scaled distances (1 < Z (m/kg$^{1/3}$)). The positive phase impulse values computed by different researchers show different tendencies in different regions. The positive phase impulse values computed from the equation of Kinney and Graham (Eq. (48)) is in close agreement with that of UFC 3-340-02. Henrych's equation (Eq. (46)) values are the largest, while the Kinney and Graham's equation (Eq. (48)) yields the smallest values among all the presented equations.

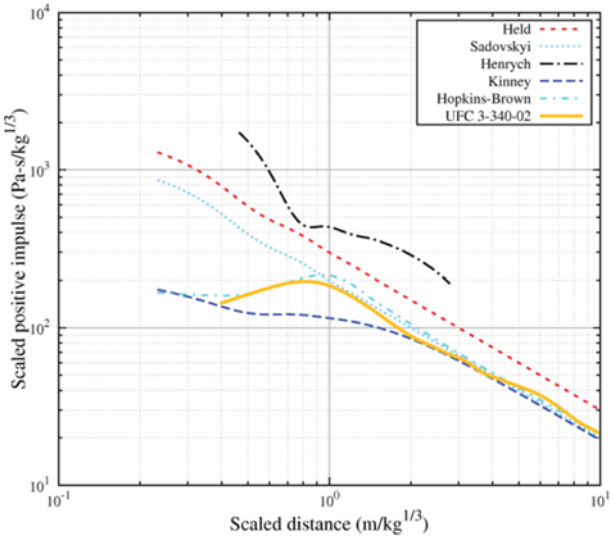

Fig. 10. Comparison of Scaled Positive Phase Impulse Computed by Empirical Formulae and UFC 3-340-02

4.1.5 Wave Decay Parameter

The wave decay parameter (b) of the modified Friedlander equation describes the shape of the temporal pressure profile. This parameter is dimensionless unlike other blast wave parameters, and influences on the length of the negative phase although the modified Friedlander equation describes only positive phase. The negative phase is important when the value of the wave decay parameter is less than one but becomes less significant for wave decay parameters greater than one (Kadid, Nezzar and Yahiaoui, 2012). Several empirical relations are summarized below:

Kinney and Graham (1985) (Kinney and Graham, 1985)

The relationship between blast impulse and the decay parameter can be expressed as:

$$\frac{i_s}{A} = \text{Impulse} = \int_0^{t_d} p\,dt = P_s t_d \left[\frac{1}{b} - \frac{1}{b^2}\left(1 - e^{-b}\right)\right] \tag{51}$$

Dharaneepathy (1993) (Dharaneepathy, 1993)

$$b = 3.18Z^{-0.58} \tag{52}$$

Lam *et al*. (2004) (Lam *et al*., 2004)

$$b = Z^2 - 3.7Z + 4.2 \tag{53}$$

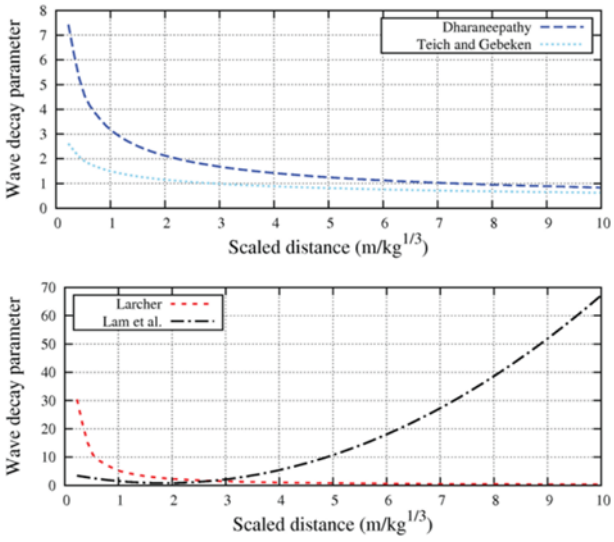

Fig. 11. Wave Decay Parameter Versus Scaled Distances

Larcher (2008) (Larcher, 2008; Kangarlou, 2013)

$$b = 5.2777Z^{-1.1975} \tag{54}$$

Teich and Gebekken (Kangarlou, 2013)

$$b = 1.5Z^{-0.38} \quad \text{for}(0.1 < Z < 30) \tag{55}$$

Figure 11 shows the relationship of wave decay parameter versus scaled distance (Z). The curves for wave decay parameter given by the researchers show different trends.

4.2 Negative Phase/Rarefaction Wave

For the negative phase or the partial vacuum phase, after the positive phase duration (t_d), the pressure decreases below the reference pressure to the maximum negative pressure (P_s^-), and then returns back to the normal atmospheric pressure (P_o) in time (t_d^-), giving a negative phase impulse (i_s^-). The maximum negative pressure or underpressure (P_s^-) has much smaller amplitude than the positive overpressure, while the negative phase duration (t_d^-) is much longer than the positive phase duration (t_d). The negative phase pressure variation versus time can be expressed as follows (Brode, 1955; Nassr, 2012):

$$P(t) = P_o - P_s^- \left(\frac{t}{t_d^-}\right)\left(1 - \frac{t}{t_d^-}\right) e^{-4t/t_d^-} \tag{56}$$

where P_o is the ambient pressure, P_s^- is the peak negative phase overpressure, t_d^- is the duration of the negative phase, and t is the time measured from the end of the positive phase duration (t_a+ t_d). Larcher (2008) presented a piecewise equation to approximate the form of the negative phase (Larcher, 2008):

$$P(t) = \begin{cases} P_o - \dfrac{2P_s^-}{t_d^-}(t - t_d) & \text{for}\left(t_d < t < t_d + \dfrac{t_d^-}{2}\right) \\ P_o - \dfrac{2P_s^-}{t_d^-}(t_d + t_d^- - t) & \text{for}\left(t_d + \dfrac{t_d^-}{2} < t < t_d + t_d^-\right) \\ P_o & \text{for}\left(t > t_d + t_d^-\right) \end{cases} \tag{57}$$

Figure 12(a) and (b) show the negative phase shock wave parameters for spherical and hemispherical explosions in free air and on the surface (Unified Facitilities Criteria 3-340-02, 2008).

4.2.1 Underpressure

The shock wave is followed by a rarefaction wave. It follows from its nature that:

$$0 < P_s^- < P_o \tag{58}$$

Following are different empirical relations for underpressure (P_s^-) in the units of megapascals (MPa). The size of the negative pressure as well as the duration of the negative part can be taken from a diagram by Drake (also shown in Krauthammer, 2008 (Krauthammer, 2008)). Drake used experimental data to obtain the mentioned diagram. The diagram can be approximated by (Larcher, 2008; Cabello, 2011):

$$P_s^- = \begin{cases} \dfrac{0.035}{Z} & \text{for}(Z > 3.5) \\ 0.01 & \text{for}(Z \le 3.5) \end{cases} \tag{59}$$

From the work of Brode and the experimental investigation of Henrych, the underpressure can be written as (Henrych and Major, 1979; Mays and Smith, 1995):

$$P_s^- = -\frac{0.034335}{Z} \quad \text{for}(Z > 1.6) \tag{60}$$

Figure 13 compares the results of available empirical relations for underpressure with the value obtained from UFC 3-340-02 (2008). It should be noted that the results of empirical equations do not show good agreement with the values of UFC charts. However, both empirical relations give close values to each other for the scaled distance range (Z (m/kg$^{1/3}$) > 3.5).

4.2.2 Negative Phase Duration

The time duration in which air pressure falls below the atmospheric pressure and then returns back to the atmospheric pressure slowly is known as negative phase duration. The negative

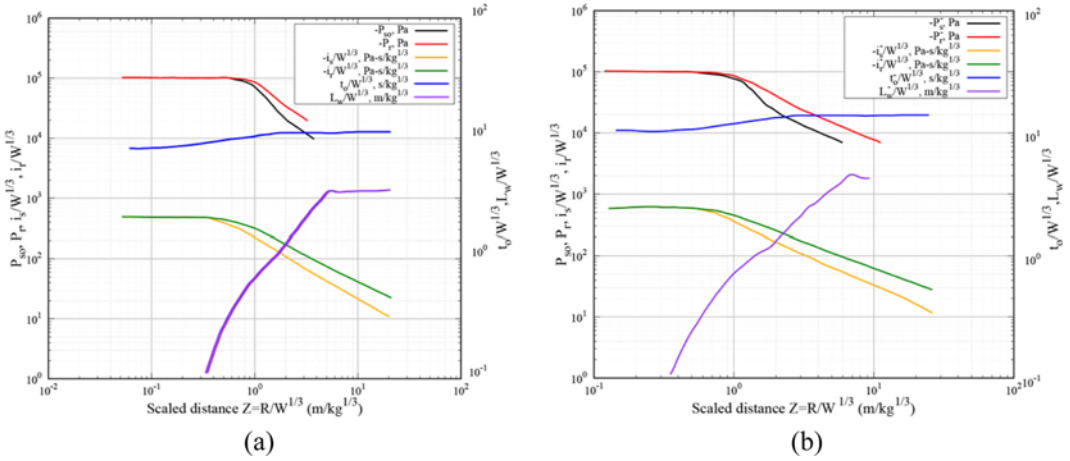

Fig. 12. Negative Phase Parameters for: (a) Spherical, (b) Hemispherical TNT Explosions

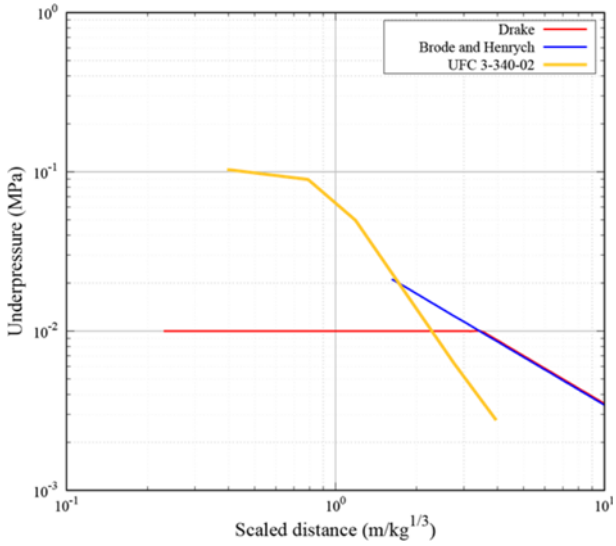

Fig. 13. Comparison of Underpressure by Empirical Formulae and UFC 3-340-02 (Fig. 12(a))

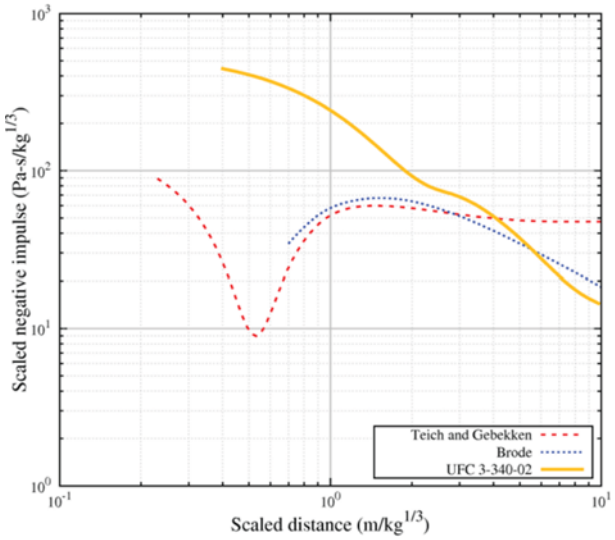

Fig. 15. Comparison of Scaled Negative Phase Impulse by Empirical Formula and UFC 3-340-02 (Fig. 12(a))

phase may last up to three times longer than the positive phase. The duration of the negative phase (t_d^-) expressed in milliseconds (ms) by Krauthammer (2008) can be described with the following equation (Larcher, 2008; Cabello, 2011):

$$t_d^- = \begin{cases} 10.4 \times W^{1/3} & \text{for } (Z < 0.3) \\ (3.125 \times \log(Z) + 12.01) \times W^{1/3} & \text{for } (0.3 \le Z \le 1.9) \\ 13.9 \times W^{1/3} & \text{for } (1.9 < Z) \end{cases} \quad (61)$$

From the theoretical work of Brode and the experimental investigation of Henrych, time duration of the negative pressure can be calculated by (Cabello, 2011):

$$t_d^- = 1.25 \times W^{1/3} \text{ (milliseconds)} \quad (62)$$

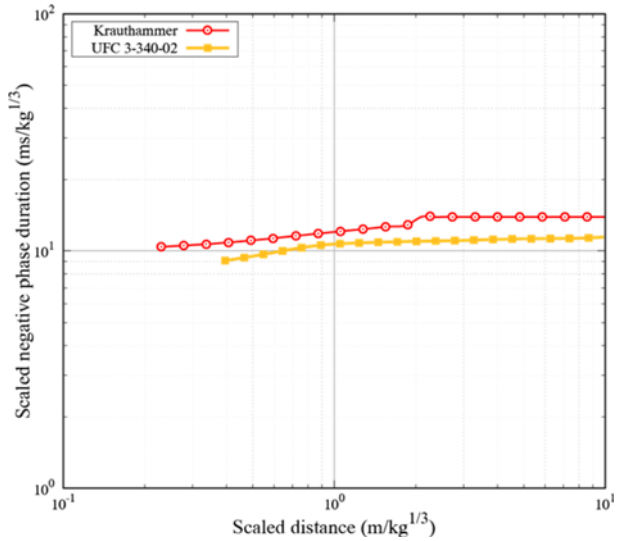

Fig. 14. Comparison of Scaled Negative Phase Duration by Empirical Equation and UFC 3-340-02 (Fig. 12(a))

Teich and Gebbeken presented the following equation to compute the time at which maximum negative pressure occurs (Goel *et al*., 2012):

$$t_{d-peak}^- = \frac{b+1}{b} t_d \quad (63)$$

Figure 14 shows the comparison of negative phase duration computed from the empirical equation of Krauthammer (Eq. (61)) with that of UFC 3-340-02. There is a very small difference in the estimation of the negative phase duration.

4.2.3 Negative Phase Impulse

The area under the negative phase of the pressure time profile is called as the negative phase impulse or underpressure impulse. Teich and Gebbeken presented the following equation to compute the underpressure impulse (Goel *et al*., 2012):

$$i_s^- = \frac{P_s t_d}{b^2} e^{-b} \quad (64)$$

Brode's solution for specific impulse in this phase (i_s^-) is given by (Mays and Smith, 1995):

$$i_s^- = i_s \left[1 - \frac{1}{2Z} \right] \quad (65)$$

Figure 15 illustrates the comparison of results by empirical relations and UFC 3-340-02. Large difference of the impulse is observed for the range of ($2 < Z$ (m/kg$^{1/3}$)), and the results get closer to each other in the scaled distance range of ($2 < Z$ (m/kg$^{1/3}$)<6).

5. Examples of Positive and Negative Blast Profiles

In this section, an example of a blast wave profile is presented using the blast wave parameters recommended in the above

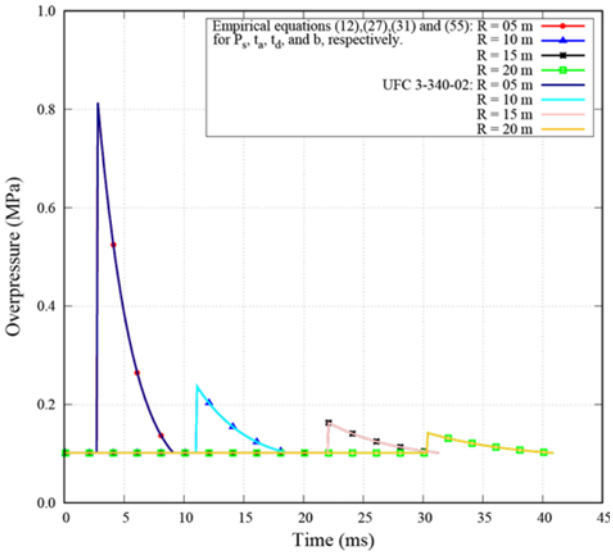

Fig. 16. Comparison of Positive Pressure Profiles by Empirical Equations and UFC 3-340-02

sections. Among many available equations, several empirical equations that show good agreement with UFC 3-340-02 are selected. Fig. 16 shows the plot of modified Friedlander equation (Eq. (5)). In this equation, the empirical equations proposed by Kinney and Graham (Eq. (12)), Wu and Hao (Eq. (27)), Sadovskyi (Eq. (31)), and Teich and Gebekken (Eq. (55)) are used for overpressure (P_s), arrival time (t_a), positive phase duration (t_d) and wave decay parameter (b), respectively. Empirical equations of overpressure (P_s), arrival time (t_a), and positive phase duration (t_d), which most reflect the UFC chart, are selected among the equations presented. However, wave decay parameter (b) is not presented in the UFC chart. Therefore the most recent empirical equation is used in the example.

The positive pressure profiles by using given empirical relations for the standoff distances R = 5, 10, 15, 20 m and the TNT charge weight W = 80 kg are compared with the profile by UFC. The pressure values are very similar, but large variations are observed in the arrival time and in the positive phase duration.

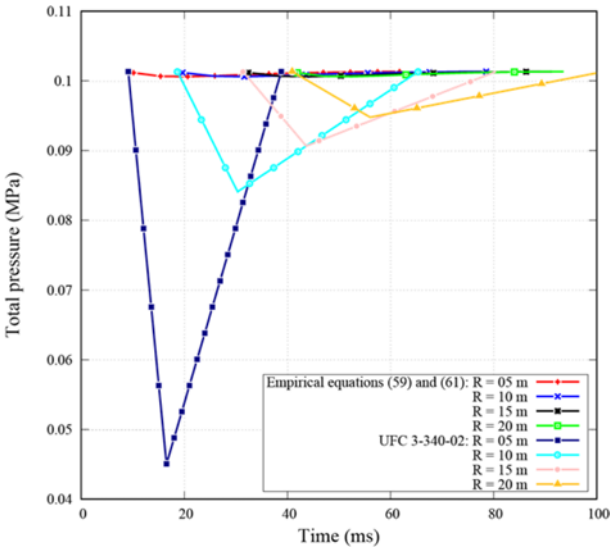

Fig. 17. Comparison of Negative Pressure Profiles by Empirical Equations and UFC 3-340-02

There are few empirical relations available in literature for negative phase of blast wave, but they do not show good agreement with the result obtained by UFC 3-340-02. Fig. 17 shows the plot of Eq. (56). for negative phase profile. In this equation, the empirical equations of Drake (Eq. (59)) and Krauthammer (Eq. (61)) are used to calculate the underpressure (P_s^-) and the negative phase duration (t_s^-), respectively, and the shapes are triangular as UFC suggests to use. The negative pressure-time curve of UFC has a time of rise equal to 0.25 times of negative phase duration (t_s^-). It should be noted that UFC shows larger values for underpressure as compared to the results produced from the given empirical relations.

6. Conclusions

This review provides a comprehensive overview of the empirical equations and blast wave parameters given by various researchers. Positive and negative incident blast wave parameters such as temporal pressure profiles, positive peak overpressures, shock arrival times, positive phase durations, positive phase impulses, and wave decay parameters are compared with those by Unified Facility Criteria (Unified Facitilities Criteria 3-340-02, 2008).

Typically, it is observed that blast parameters at large distances from an explosive charge can be predicted accurately using the presented equations. However, if the explosive is very close to the target, the accuracy might decrease since there are limited test data available that might be used to validate the parameters for near regions (Bogosian and Heidenreich, 2012). Especially, in the negative phase of the blast wave, the results show large difference compared with the result by UFC. One possible reason of this variation is that the experimental data contain weather effects of the explosive performance in the real world conditions, but those are not included in the equations up till now (Swisdak Jr., 1994). Therefore, appropriate care and judgment are required in applying any of these empirical relations to a real situation. Various types of comparison of the presented equations against test data and improvement of the empirical formulae are important to enhance the reliability of the given equations.

Based on the comparative study of several dozens of the presented empirical equations, the most appropriate equations are selected to compute the incident blast wave parameters. These suggested equations give values closer to that of UFC curves, or they are the only available choices. For example, in case of negative phase, we do not have many choices available to select. The peak overpressure (P_s) and positive phase impulse (i_s) can be calculated using the equations by Kinney and Graham (Eq. (12)) and Kinney and Graham (Eq. (48)), respectively. Additionally, the shock arrival time (t_a), the positive phase

duration (t_d) and the wave decay parameter (b) can be obtained using the equations by Wu and Hao (Eq. (27)), Sadovskyi (Eq. (31)), and Teich and Gebekken (Eq. (55)), respectively. Similarly, the negative phase parameters can be calculated using the equations by Drake (Eq. (59)), Krauthammer (Eq. (61)), and Brode (Eq. (65)), respectively.

Acknowledgements

This research was supported by a grant from a Construction Technology Research Project (Development of impact/blast resistant HPFRCC and evaluation technique thereof, 13SCIPS02) funded by the Ministry of Land, Infrastructure, and Transport, and was also supported by U-city Master and Doctor Course Grant Program of Korea Ministry of Land, Infrastructure and Transport (MOLIT).

References

Abdollahzadeh, G. and Nemati, M. (2013). "Risk assessment of structures subjected to blast." *Int. J. Damage Mech.*, Vol. 23, No. 1, pp. 3-24, DOI: 10.1177/1056789513482479.

Adushkin, V. V. and Korotkov, A. I. (1961). "Parameters of a shock wave near to HE charge at explosion in air." *PMTF*, Vol. 5, pp. 119-123.

Ahmad, S., Elahi, A., Pervaiz, H., Rahman, A. G. A., and Barbhuiya, S. (2014). "Experimental study of masonry wall exposed to blast loading." *Materiales de Construccion*, Vol. 64, No. 313, pp. 1-11, DOI: 10.3989/mc.2014.01513.

Ahmad, S., Taseer, M., and Pervaiz, H. (2012). "Effects of impulsive loading on reinforced concrete structures." *Tech. J., Univ. Eng and Technol. Taxila, Pakistan* (Vibration analysis issue).

Bajić, Z. (2007). "Determination of TNT equivalent for various explosives." Master's, University of Belgrade, Belgrade, Serbia.

Bangash, M. Y. H. and Bangash, T. (2006). *Explosion-resistant buildings*, Springer, London, UK.

Beshara, F. B. A. (1994). "Modelling of blast loading on aboveground structures—I. General phenomenology and external blast." *Comput. and Struct.*, Vol. 51, No. 5, pp. 585-596, DOI: 10.1016/0045-7949 (94)90066-3.

Bogosian, D. D. and Heidenreich, A. N. (2012). "An evaluation of engineering methods for predicting close-in air blast." *Proc., Structures Congress 2012*, pp. 90-101, DOI: 10.1061/9780784412367.009.

Brode, H. L. (1955). "Numerical solutions of spherical blast waves." *J. Appl. phys.*, Vol. 26, No. 6, pp. 766-775, DOI: 10.1063/1.1722085.

Cabello, B. (2011). *Dynamic stress analysis of the effect of an air blast wave on a stainless steel plate*, Master's thesis, Rensselaer Polytechnic Institute Hartford, Connecticut.

Chang, D. B. and Young, C. S. (2010). "Probabilistic Estimates of vulnerability to explosive overpressures and impulses." *J. Phys. Secur.*, Vol. 4, No. 2, pp. 1-29.

Chock, J. M. K. (1999). *Review of Methods for Calculating Pressure Profiles of Explosive Air Blast and its Sample Application*. Mater's thesis, Virginia Polytechnic Institute and State University, Blacksburg, Virginia.

Conrath, E. J. (1999). *Structural design for physical security: State of the practice*, ASCE Publications.

Cranz, C. (1926). *Lehrbuch der Ballistik*, II Band. Berlin.

De Silva, C. W. (2010). *Vibration and shock handbook*, CRC Press, USA.

Dharaneepathy (1993). *Air-blast effects on shell structures*, Phd thesis, Anna University, Madras.

Esparza, E. D. (1986). "Blast measurements and equivalency for spherical charges at small scaled distances." *Int. J. Impact Eng.*, Vol. 4, No. 1, pp. 23-40, DOI: 10.1016/0734-743X(86)90025-4.

Gelfand, B. and Silnikov, M. (2004). *Translation from Russian to English the Book "Blast Effects Caused by Explosions"*, DTIC Document, London, England.

Goel, M. D., Matsagar, V. A., Gupta, A. K., and Marburg, S. (2012). "An abridged review of blast wave parameters." *Def. Sci. J.*, Vol. 62, No. 5, pp. 300-306, DOI: 10.14429/dsj.62.1149.

Held, M. (1983). "Blast waves in free air." *Propellants, Explos., Pyrotech.*, Vol. 8, No. 1, pp. 1-7, DOI: 10.1002/prep.19830080102.

Henrych, J. and Major, R. (1979). *The dynamics of explosion and its use*, Elsevier, Amsterdam.

Hopkins-Brown, M. A. and Bailey, A. (1998). Chapter 2 (Explosion Effects) Part 1., *AASTP-4* Royal Military College of Science, Cranfield University.

Hopkinson, B. (1915). *British ordnance board minutes,* Rep, 13565.

Iqbal, J. and Ahmad, S. (2011). "Improving safety provisions of structural design of containment against external explosion." *Proc. International conference on opportunities and challenges for water cooled reactors in the 21st century*, Intenational Atomic Energy Agency (IAEA).

Izadifard, R. A. and Foroutan, M. (2010). "Blastwave parameters assessment at different altitude using numerical simulation." *Turk. J. Eng. and Environ. Sci.*, Vol. 34, No. 1, pp. 25-42, DOI: 10.3906/muh-0911-39.

Jeremić, R. and Bajić, Z. (2006). "An approach to determining the TNT equivalent of high explosives." *Sci. Tech. Rev.*, Vol. 56, No. 1, pp. 58-62.

Kadid, A., Nezzar, B., and Yahiaoui, D. (2012). "Nonlinear dynamic analysis of reinforced concrete slabs subjected to blast loading." *Asian J. Civ. Eng. (Build. and Hous.)*, Vol. 13, No. 5, pp. 617-634.

Kangarlou, K. (2013). "Mechanics of blast loading on the head models in the study of traumatic brain injury." *Nationalpark-Forschung In Der Schweiz (Switz. Res. Park J.)*, Vol. 102, No. 11, pp. 1571-1581.

Kim, J. H. J., Yi, N. H., Kim, S. B., Choi, J. K., and Park, J. C (2009). "Experiment study on blast loading response of FRP-retrofitted RC slab structures." *Proc., Asia-Pacific Conference on FRP in Structures*, pp. 533-538.

Kingery, C. N. and Bulmash, G. (1984). *Air blast parameters from TNT spherical air burst and hemispherical surface burst*, Ballistic Research Laboratories.

Kinney, G. F. and Graham, K. J. (1985). *Explosive shocks in air*, Springer-Verlag, Berlin and New York.

Krauthammer, T. (2008). *Modern protective structures*, CRC Press, USA.

Lam, N., Mendis, P., and Ngo, T. (2004). "Response spectrum solutions for blast loading." *Electron. J. Struct. Eng.*, Vol. 4, pp. 28-44.

Larcher, M. (2008). *Pressure-time functions for the description of air blast waves,* Technical note, JRC.

Li, J. and Ma, S. (1992). *Explosion mechanics*, Science Press, Beijing.

Low, H. Y. and Hao, H. (2001). "Reliability analysis of reinforced concrete slabs under explosive loading." *Struct. Saf.*, Vol. 23, No. 2, pp. 157-178, DOI: 10.1016/S0167-4730(01)00011-X.

Mays, G. C. and Smith, P. D. (1995). *Blast effects on buildings: design of buildings to optimize resistance to blast loading*, Thomas Telford, London.

Mills, C. A. (1987). "The design of concrete structure to resist explosions and weapon effects." *Proceedings of the 1st Int. Conference on Concrete for Hazard Protections*, pp. 61-73.

Nassr, A. A. (2012). *Experimental and analytical study of the dynamic response of steel beams and columns to blast loading*, Open Access Dissertations and Theses, McMaster University, Hamilton, Canada.

Newmark, N. M. and Hansen, R. J. (1961). Design of blast resistant structures, *Shock and vibration handbook*, Harris, and Crede, eds., McGraw-Hill, New York, USA.

NFPA (2008). *Guide to fire and explosion investigations NFPA 921*, National Fire Protection Association, Quincy, Massachussetts.

Pape, R., Mniszewski, K. R., and Longinow, A. (2009). "Explosion phenomena and effects of explosions on structures. I: Phenomena and effects.: *Pract. Period. Struct. Des. and Constr.*, Vol. 15, No. 2, pp. 135-140, DOI: 10.1061/(ASCE)SC.1943-5576.0000038 .

Pierre-Emmanuel S. (2012). Etude des phénomènes physiques associés à la propagation d'ondes consécutives à une explosion et leur interaction avec des structures, dans un environnement complexe. Autre. Université d'Orléans, Français.

Sachs, R. G. (1944). *Dependence of blast on ambient pressure and temperature*, BRL-466 Ballistic Research Laboratory, Aberdeen, Maryland.

Sadovskiy, M. A. (2004). *Mechanical effects of air shock waves from explosions according to experiments, Selected works: Geophysics and physics of explosion*, Nauka Press, Moscow.

Saska, P., Krzystała, E., and Mężyk, A. (2011). "An analysis of an explosive shock wave impact onto military vehicles of contemporary warfare." *J. KONES*, Vol. 18, No. 1, pp. 515-524.

Smith, P. D. and Hetherington, J. G. (1994). *Blast and ballistic loading of structures*, Butterworth-Heinemann Oxford, UK.

Swisdak Jr., M. M. (1994). *Simplified Kingery airblast calculations*, Minutes of the Twenty Sixth DOD Explosives Safety Seminar, DTIC Document, Maryland.

Uddin, N. (2010). *Blast protection of civil infrastructures and vehicles using composites*, Elsevier, New York, USA.

UFC (2008). *Unified Facilities Criteria 3-340-02: Structures to resist the effects of accidental explosions*, Dept. of the Army, the NAVY and the Air Force, Washington DC, USA.

UNODA (2011). *Formulae for ammunition management IATG 01.80*, United Nations Office for Disarmament Affairs (UNODA), New York, USA.

Vijayaraghavan, C., Thirumalaivasan, D., and Venkatesan, R. (2012). "A study on nuclear blast overpressure on buildings and other infrastructures using geospatial technology." *J. Comput. Sci.*, Vol. 8, No. 9, pp. 1520-1530, DOI: 10.3844/jcssp.2012.1520.1530.

Wu, C. and Hao, H. (2005). "Modeling of simultaneous ground shock and airblast pressure on nearby structures from surface explosions." *Int. J. Impact Eng.*, Vol. 31, No. 6, pp. 699-717, DOI: 10.1016/j.ijimpeng.2004.03.002.

Yin, X., Gu, X., Lin, F., and Kuang, X. (2009). *Numerical analysis of blast loads inside buildings*, Computational Structural Engineering, Springer, Netherlands, pp. 681-690.